

# Evaluating the long-term behaviour and viability of an oil sands tailings management and reclamation strategy

HL Cossey *University of Alberta, Canada*

H Kaminsky *Northern Alberta Institute of Technology, Canada*

AC Ulrich *University of Alberta, Canada*

## Abstract

*Surface mining of oil sands ore in Alberta, Canada, has generated over a billion cubic metres of waste, known as fluid fine tailings (FFT). FFT are a mixture of fine-grained solids (silt and clay), water, dissolved salts, and organic compounds. Eventually, FFT must be reclaimed and integrated into mine closure landscapes. One proposed method of FFT management and reclamation is through end pit lakes (EPLs), which are engineered water bodies that consist of a thick layer of FFT capped with water. FFT deposited in EPLs may also be treated with a coagulant (alum) and polymer flocculant (polyacrylamide, PAM) to improve tailings dewatering and cap water quality. Theoretically, EPLs are a suitable reclamation strategy because the water cap develops into habitat for an aquatic ecosystem while the FFT slowly dewater over time. However, successful use of EPLs in the oil sands has not been demonstrated, and knowledge gaps exist surrounding the long-term behaviour of EPLs and their viability as an FFT management and reclamation strategy. Uncertainties surrounding EPL behaviour include the flux of salts and organics into the water cap, biogeochemical cycling processes, which can generate sulfide species and greenhouse gases, and the environmental fate of PAM. To address these knowledge gaps, aging experiments are being performed in 1 L and 19 L EPL columns containing untreated or treated (with alum and PAM) FFT and a water cap. Aging is simulated in the columns through higher temperature and carbon amendments. Results to date show that fluxes of salts into the water caps are generally consistent with consolidation trends and are similar in columns containing either untreated or treated FFT. Compared to untreated FFT, treated FFT has undergone more extensive sulfur cycling, as evidenced by higher sulfate reduction rates and higher sulfide species concentrations.*

**Keywords:** *mine waste management, end pit lakes, biogeochemistry, sulfur cycling, consolidation, salt fluxes, polyacrylamide*

## 1 Introduction

Over 1.4 billion m<sup>3</sup> of waste, known as fluid fine tailings (FFT), has been generated from oil sands surface mining in Alberta, Canada (Alberta Energy Regulator [AER] 2021). FFT consists of fine-grained solids (silt and clay), residual heavy oil (bitumen), and process-affected water that contains various chemical constituents and organic compounds. Eventually, all the FFT must be reclaimed and integrated into mine closure landscapes. End pit lakes (EPLs) are a proposed FFT management and reclamation method in which 10–80 m of FFT are capped with 3–10 m of water in decommissioned open pits (Cossey et al. 2021a). Currently, oil sands EPL technology is being tested by two companies: Syncrude Canada Ltd (Syncrude) and Suncor Energy Inc. (Suncor). Syncrude has a demonstration-scale EPL, the Syncrude Demonstration Pond, and a full-scale 800 ha EPL called Base Mine Lake (BML), which contains approximately 45 m of untreated FFT and a 9 m water cap (Canada's Oil Sands Innovation Alliance [COSIA] 2021; Syncrude Canada Ltd 2021). Suncor is investigating a tailings treatment technology called permanent aquatic storage structure (PASS) in which FFT is first treated with a coagulant (alum) and a polymer flocculant (polyacrylamide, PAM) before being deposited in an EPL. The intention of PASS is to improve tailings dewatering and release water quality (COSIA 2021). The PASS technology is currently being evaluated at Suncor's 18 ha pilot-scale demonstration EPL called Lake Miwasin and at Dedicated Disposal Area 3 (DDA3) (COSIA 2021). Although EPLs have not yet

been approved as an oil sands tailings reclamation technology, an estimated 11 EPLs will be created for tailings reclamation and will eventually be incorporated into Alberta's oil sands closure landscapes (COSIA 2021).

FFT reclamation is challenging as it can take decades for FFT to naturally consolidate (dewater) because of the stability of the clay water slurry (Chalaturnyk et al. 2002). As such, EPLs were proposed as an FFT management practice and reclamation strategy because the FFT can slowly dewater over time, while the water cap serves as habitat for aquatic ecosystems. The end goal is for EPLs to become lake ecosystems; however, successful use of oil sands EPLs in this capacity has not been demonstrated, and knowledge gaps exist surrounding the long-term behaviour of EPLs and their viability as a tailings reclamation strategy.

EPLs are still in the technology validation phase in the oil sands, with Syncrude's BML being the most developed at 10 years old. Studies of BML have found that expressed salts (predominantly sodium,  $\text{Na}^+$ , and chloride,  $\text{Cl}^-$ ) and organics (including residual bitumen and toxic organic acids called naphthenic acid fraction compounds (NAFCs)) are influencing water cap quality; without manual intervention, BML may eventually resemble a brackish or estuarine ecosystem with less biodiversity (Brown & Ulrich 2015; Monaghan et al. 2021; Rundle et al. 2018; Syncrude Canada Ltd 2020; White & Liber 2018, 2020). The implications of PASS technology on contaminant fluxes and water cap quality, if any, must also be evaluated.

FFT in EPLs will also undergo various biogeochemical cycling processes, depending on the abundance of electron acceptors. Numerous FFT deposits, including BML, have been found to generate greenhouse gases (carbon dioxide ( $\text{CO}_2$ ) and methane ( $\text{CH}_4$ )) mainly through a microbial process known as methanogenesis (Clark et al. 2021; Small et al. 2015). However, because of the alum addition in PASS, sulfur cycling is also likely to be a dominant biogeochemical cycling process in PASS-treated FFT. Previous studies have reported extensive sulfate reduction in similarly sulfate-amended FFT deposits, resulting in the generation of aqueous and gaseous hydrogen sulfide ( $\text{H}_2\text{S}$ ) (Reid & Warren 2016; Warren et al. 2016). Additionally, alum was added to the BML water cap in 2016, resulting in the generation of aqueous sulfide species near the FFT-water interface and a shift in microbial communities, including the appearance of sulfate-reducing bacteria (Jessen et al. 2022). As such, the implications of PASS treatment on biogeochemical cycling processes, particularly sulfur cycling, in EPLs must be evaluated. Further, the environmental fate and biodegradation of PAM in PASS-treated FFT and its impacts on FFT stability remain largely unknown.

The objective of this research is to address these knowledge gaps by accelerating the EPL aging process in 40 laboratory-scale columns. Each column has been set up to mimic an EPL and contains either untreated or PASS-treated tailings and a water cap. Monitoring the evolution of these columns over time will elucidate the potential biogeochemical and geotechnical behaviour of untreated and PASS-treated FFT in EPLs.

## 2 Methodology

### 2.1 Aging methodology

As oil sands tailings age, they undergo microbially derived biogeochemical cycling processes and consolidation processes. Anaerobic microbial activity, most commonly methanogenesis and sulfate reduction, in FFT can lead to biodegradation of organics, mineral transformations, and biogenic gas emissions of  $\text{CO}_2$ ,  $\text{CH}_4$ , and  $\text{H}_2\text{S}$  (Clark et al. 2021; Gee et al. 2017; Siddique et al. 2006, 2007, 2011, 2014a, 2015, 2020; Small et al. 2015; Stasik et al. 2014). Further, microbial activity can also enhance consolidation (known as bioconsolidation) through the ebullition and dissolution of biogenic gases (Siddique et al. 2014b).

To evaluate the long-term behaviour of EPLs in the laboratory in a timely manner, two methods are being used to simulate and accelerate these biogeochemical and bioconsolidation processes: elevated temperature and hydrocarbon amendments. Elevated temperatures (up to an optimum temperature) increase microbial metabolic rates (Pavlostathis & Zhuang 1991), while hydrocarbons act as electron donors or substrates for microbial degradation processes. Based on the work of Wong et al. (2015) and Siddique et al. (2014b), an incubation temperature of  $20^\circ\text{C}$  was selected to increase microbial metabolic rates in FFT. A control temperature of  $10^\circ\text{C}$  was chosen as it is roughly consistent with the average annual temperature of FFT in

BML (Dompierre et al. 2016; Tedford et al. 2019). Hydrocarbon amendments used in this work include BTEX (benzene, toluene, ethylbenzene and xylenes) components, as well as select *n*-alkanes and iso-alkanes, all of which can be degraded by microorganisms found in FFT. Methanogens can degrade numerous hydrocarbons, including BTEX, *n*-alkanes, and iso-alkanes (Siddique et al. 2006, 2007, 2011, 2020), and sulfate-reducing bacteria can degrade light hydrocarbons such as BTEX (Stasik & Wendt-Potthoff 2014). The elevated temperature and hydrocarbon amendments used in this work will accelerate microbial activity and subsequent biogeochemical cycling and bioconsolidation processes that have been observed in numerous tailings ponds and deposits, including BML (Dompierre et al. 2016; Ramos-Padrón et al. 2011; Reid & Warren 2016; Stasik & Wendt-Potthoff 2014; Warren et al. 2016). Further, the addition of hydrocarbons also provides an indication of biogeochemical cycling and bioconsolidation processes that may be important in froth treatment tailings, which are also generated during bitumen extraction from oil sands ore, although froth treatment tailings differ from FFT in that they contain residual diluent (most commonly naphtha). Because froth treatment tailings contain additional hydrocarbons, they are more likely to trigger microbial processes; for example, tailings ponds that contain froth treatment tailings have the highest methane production (Burkus et al. 2014).

## 2.2 Experimental set-up

### 2.2.1 Sample collection and treatment

Approximately 400 L of untreated FFT was collected from an oil sands tailings pond in 2019. The FFT was homogenised and subsampled into 20 L pails at the Northern Alberta Institute of Technology (NAIT) (Edmonton, CA). Half of the FFT was transferred to the University of Alberta (Edmonton, CA) to be stored at 4°C until use; the other half was first treated at NAIT before being transferred to the University of Alberta. Treatment involved adding a coagulant, alum ( $\text{Al}_2(\text{SO}_4)_3 \cdot 14\text{H}_2\text{O}$ ), and partially hydrolysed anionic polymer flocculant, PAM, and shearing the treated FFT via a conveyance test. The alum and PAM doses were approximately 875 mg/L of porewater and 2.43 g/kg of solids, respectively. NAIT's flocculation procedure (see Li et al. 2021a) and conveyance test (see Li et al. 2021b, 2022) mimic Suncor's PASS treatment process and the subsequent mechanical shearing that occurs during pipeline transport of the PASS-treated FFT to a disposal area.

Freshwater from Beaver Creek Reservoir (BCR), which is the freshwater source for BML, was used for the water cap. BCR water was collected in 20 L pails in 2015 and stored at 4°C at the University of Alberta until use. BCR water was selected for this work because its water chemistry is similar to that of the Athabasca River, which will likely be hydrologically connected to future oil sands EPLs in northern Alberta (Cossey et al. 2021a; Government of Alberta 2022).

### 2.2.2 Column experiments

#### 2.2.2.1 Column set-up

Table 1 presents a summary of the 40 columns set up for this experiment. Sixteen 19 L columns were set up in duplicate, and 24 1 L columns were set up in triplicate. Each column contains either untreated FFT or PASS-treated FFT (hereinafter referred to as PASS) and a freshwater cap. The tailings-to-water cap ratio in each column was 2.5:1 to ensure sufficient volumes of both tailings and water for sample collection throughout the experiment. As such, the 19 L columns contain 12.5 L of tailings, 5 L of BCR water, and 1.5 L of headspace, and the 1 L columns contain 0.75 L of tailings, 0.3 L of BCR water, and 0.13 L of headspace. The column set-up is illustrated in Figure 1 (note that these photos were taken on Day 120 of the aging experiment). The columns were set up in June 2021 and will be continuously monitored for 1.5 years.

**Table 1 Summary of 40 columns set up for aging experiments. 19 L columns labelled as B (for big) are set up in duplicate; 1 L columns labelled as S (for small) are set up in triplicate**

| Column        | Temperature (°C) |    | Hydrocarbon (HC) amendments | Size (L) |    |
|---------------|------------------|----|-----------------------------|----------|----|
|               | 10               | 20 |                             | 1        | 19 |
| FFT B10       | X                |    |                             |          | X  |
| FFT B20       |                  | X  |                             |          | X  |
| FFT B10 + HC  | X                |    | X                           |          | X  |
| FFT B20 + HC  |                  | X  | X                           |          | X  |
| FFT S10       | X                |    |                             | X        |    |
| FFT S20       |                  | X  |                             | X        |    |
| FFT S10 + HC  | X                |    | X                           | X        |    |
| FFT S20 + HC  |                  | X  | X                           | X        |    |
| PASS B10      | X                |    |                             |          | X  |
| PASS B20      |                  | X  |                             |          | X  |
| PASS B10 + HC | X                |    | X                           |          | X  |
| PASS B20 + HC |                  | X  | X                           |          | X  |
| PASS S10      | X                |    |                             | X        |    |
| PASS S20      |                  | X  |                             | X        |    |
| PASS S10 + HC | X                |    | X                           | X        |    |
| PASS S20 + HC |                  | X  | X                           | X        |    |

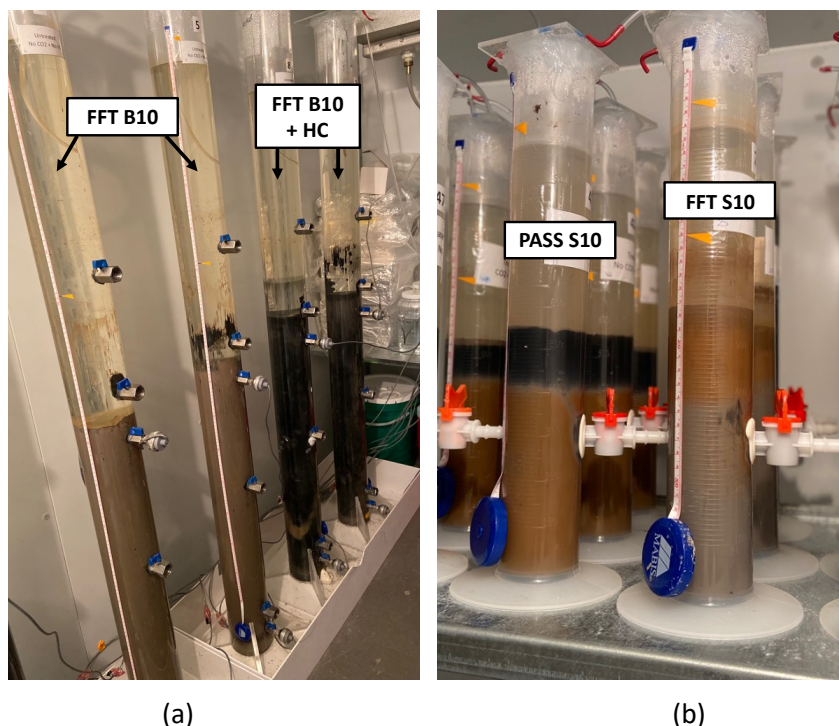


**Figure 1 (a) Two 19 L FFT columns and two 19 L FFT + hydrocarbons (HC) columns stored at 10°C; (b) 1 L FFT column and 1 L PASS column stored at 10°C. Photos were taken on Day 120**

The 19 L columns were built using 1.85 m cast acrylic tubes (Johnston Industrial Plastics Ltd, Edmonton, CA) with an inner diameter (ID) of 11.4 cm and a thickness of 0.6 cm, and a 1.3 cm thick cast acrylic sheet base (Plastics Plus Ltd, Edmonton, CA). The 1 L columns are 1 L polypropylene Fisherbrand™ graduated cylinders (3004001000, Mexico) that are 41.9 cm tall with an ID of 6.1 cm. The 19 L columns were each equipped with four sampling ports (1.9 cm stainless steel (316) mini ball valve – FxM NPT, Direct Material, Irving, USA) for measuring and collecting tailings and water samples; the 1 L columns were equipped with one sampling port (1.3 cm two-way ball valve with 10 mm hose barb) for sampling tailings. Each 19 L column was also equipped with two pore pressure transducers (0 to 69 kPa, Item # RK-68075-42, Cole Parmer, Montreal, CA) that are attached to the columns with 0.6 cm ball valves (stainless steel (316) mini ball valve – FxM NPT, Direct Material, Irving, USA). All 40 columns are stored in the dark (under black tarps) and under anaerobic conditions to resemble the conditions under which tailings exist in EPLs. Each column was sealed using a 0.48 cm thick cast acrylic sheet lid (Plastics Plus Ltd, Edmonton, CA) and silicon, and was flushed with nitrogen gas immediately after the column was filled. Each lid was equipped with a septum (CLS-4209-14, butyl rubber, Chemglass) and 0.3 cm vinyl tubing (Fisher Scientific, Pittsburgh, PA, USA) to allow for water cap and headspace sampling. All columns are stored under quiescent conditions; as such, these columns cannot account for behavioural differences that may occur in the field due to wave and wind activity.

To accelerate aging, 20 of the columns (eight 19 L and 12 1 L columns) are being stored at 20°C, while the other 20 columns are stored at 10°C in a McKinley & Taylor cooler (Edmonton, CA) regulated with a Johnson Controls Inc. electronic temperature control (A419, Milwaukee, USA). The tailings in 20 of the columns were amended with hydrocarbons prior to being placed in the columns. Hydrocarbon amendments were added as a free phase to the tailings slurry and were as follows: toluene (150 ppm) ( $\geq 99.9\%$ , Sigma-Aldrich, St. Louis, USA), *o*-xylene (50 ppm) (99%, Alfa Aesar, Ottawa, CA), *m*-xylene (50 ppm) ( $>99\%$ , TCI AMERICA, Portland, USA), *p*-xylene (50 ppm) (99%, Alfa Aesar, Ottawa, CA), *n*-decane (500 ppm) (99.5%, Fisher Scientific, Fair Lawn, USA), *n*-octane (500 ppm) (99+%, Thermo Fisher Scientific, Fair Lawn, USA), 2-methylpentane (500 ppm) ( $\geq 99$ , Sigma-Aldrich, St. Louis, USA) and 3-methylhexane (500 ppm) (99%, ChemSampCo, Dallas, USA). The hydrocarbons and concentrations used were selected based on the previous work of Siddique et al. (2006, 2007, 2011, 2020) and Stasik & Wendt-Potthoff (2014).

### 2.2.2.2 Column sampling and monitoring

The tailings, water cap, and headspace in each column are being continuously monitored throughout the experiment. Interface settlement is being measured regularly to monitor settlement and consolidation behaviour of the tailings. Tailings porewater pressure is being measured every 2 h in the 19 L columns using the previously mentioned pressure transducers and a Keysight datalogger (DAQ973A Data Acquisition System and Keysight DAQM901A 20 channel multiplexers, Santa Rosa, USA). The pH, electrical conductivity (EC), and redox potential of the tailings and water cap in each column are also regularly monitored. Because the sampling ports on the 19 L and 1 L columns have different diameters, different probes are used for each size of column. In the 19 L columns, pH is measured using a Thermo Scientific Orion Dual Star pH/ISE Benchtop and an E-1325M pH probe (Gain Express); EC is measured using a Fisher Scientific Accumet AR50 Dual Channel pH/Ion/Conductivity Meter and an Atlas Scientific conductivity probe K 0.1 (Long Island City, USA); and redox potential is measured using Thermo Scientific Orion Dual Star pH/ISE Benchtop and an ORP-1 probe (Gain Express). In the 1 L columns, pH is measured using a Thomas Scientific micro pH electrode (Swedesboro, USA), EC is measured using an MI-915 conductivity electrode (Microelectrodes Inc. Bedford, USA), and redox potential is measured using a Mettler Toledo micro ORP electrode (S7, Greifensee, Switzerland).

Water cap and tailings porewater samples are collected every 60 d and 120 d, respectively, to measure major cations ( $\text{Na}^+$ ,  $\text{K}^+$ ,  $\text{Ca}^{2+}$ ,  $\text{Mg}^{2+}$ , Fe, and Al), major anions ( $\text{Cl}^-$ ,  $\text{SO}_4^{2-}$ ,  $\text{NO}_3^-$ ,  $\text{NO}_2^-$ ,  $\text{F}^-$ , and  $\text{PO}_4^{3-}$ ), aqueous total sulfide species, alkalinity, and dissolved organic carbon (DOC). Because of the small volume of tailings in the 1 L columns, tailings samples are only collected from the 19 L columns. Similarly, because of the large sample volume required for total sulfide species analysis, only the water cap samples from the 19 L columns are analysed for total sulfide species. Major cations analysis is conducted at the Natural Resources Analytical Laboratory at the University of Alberta using inductively coupled plasma – optical emission spectrometry

(ICP-OES) (Thermo iCAP 600 series, Thermo Fisher Scientific, Bremen, Germany). Major anions are analysed using a Dionex 2100 Ion Chromatography System (Thermo Scientific, Bannock, USA). Aqueous total sulfide species ( $\text{H}_2\text{S}$ ,  $\text{HS}^-$ ,  $\text{S}^{2-}$ ) are measured using the HACH Methylene Blue Method (Method 8131) in conjunction with a HACH DR 900 Multiparameter Portable Colorimeter (Loveland, USA). Total alkalinity is measured using a Metrohm Eco Titrator (Herisau, Switzerland) with 0.02 N  $\text{H}_2\text{SO}_4$  as the titrant. DOC is measured using a Shimadzu TOC-LCPH analyser (Kyoto, Japan) with the following parameters: 6 min sparging time; 50  $\mu\text{L}$  injection volume; injection number: 3 out of 4; acid added: 2.3%. Additionally, PAM was measured in water cap samples collected from the 19 L columns on Day 180. PAM is measured in 0.45  $\mu\text{m}$  filtered samples using size exclusion chromatography with an Agilent 1200 Infinity Series High Performance Liquid Chromatography (Santa Clara, USA). An Agilent PL Aquagel-OH Mixed-H column (8  $\mu\text{m}$ , 300  $\times$  7.5 mm) (Santa Clara, USA) was used with a 0.01 M  $\text{NaH}_2\text{PO}_4$  + 0.1 M  $\text{NaCl}$  mobile phase, neutral pH, and a flow rate of 0.75 mL/min.

Biogenic gas emissions are being monitored by measuring headspace concentrations of  $\text{CO}_2$ ,  $\text{CH}_4$ , and  $\text{H}_2\text{S}$ .  $\text{CO}_2$  and  $\text{CH}_4$  are measured every 30 d through manual injection gas chromatography with a flame ionisation detector (Agilent 7890A+/5977B GC-MS, Santa Clara, USA). Headspace  $\text{H}_2\text{S}$  concentrations in the 16 19 L columns are measured every 180 d at AGAT Laboratories (Calgary, CA) using gas chromatography with a sulfur chemiluminescence detector. To further analyse microbial activity, tailings samples are collected every 120 d for DNA extraction with a FastDNA™ Spin Kit for Soils (MP Biomedical Solon, USA). DNA samples are sent to High Content Analysis Core at the University of Alberta for polymerase chain reaction amplification of the V3 and V4 regions of the 16S rRNA gene from bacteria and archaea (using forward primer 5'-TCGTCCGACGTCAGATGTGTATAAGAGACAGCCTACGGGNGGCWGCAG-3' and reverse primer 5'-GTCTCGTGGGCTCGGAGATGTGTATAAGAGACAGGACTACHVGGGTATCTAATCC-3'). Subsequent amplicon sequencing is conducted with the Illumina PE250 platform (Illumina, San Diego, USA).

The initial (Day 0) samples of untreated FFT, PASS, and BCR water were also analysed for pH, EC, major cations and anions, aqueous total sulfide species, total alkalinity, DOC, and NAFCs. NAFCs were extracted and measured using Fourier-transform infrared spectrometry (FTIR) (Spectrum 100 FTIR Spectrometer, PerkinElmer, Shelton, USA) following the procedure outlined in Ripmeester & Duford (2019). The untreated FFT and PASS samples were further analysed for solids content and water content. Methylene blue index (MBI) and bitumen content were measured in the untreated FFT only, and these two parameters are assumed to be the same in PASS-treated FFT as in the original untreated FFT. MBI was measured at NAIT following the method in Kaminsky (2014) and bitumen content was also measured at NAIT using Dean–Stark analysis. Finally, the particle-size distribution of the untreated FFT was determined using a sedimentation (hydrometer) test. Particle-size distribution was conducted in accordance with ASTM International D7928-17: Standard Test Method for Particle-Size Distribution (Gradation) of Fine-Grained Soils Using the Sedimentation (Hydrometer) Analysis (ASTM 2017) using a 152H hydrometer (Fisherbrand, Buena, USA).

### 3 Results

This section will highlight results up to and including Day 240 of this experiment. Select geotechnical and water chemistry parameters from Day 0 characterisation of the untreated FFT, PASS, and BCR water are presented in Table 2; additional characterisation data can be found in Cossey et al. (2021b). The water chemistry of the untreated FFT and PASS are similar with a few exceptions. PASS porewater has a higher EC, largely caused by the addition of alum. Alum addition also results in high concentrations of sulfate in PASS ( $631.9 \pm 21.4$  mg/L) relative to that of untreated FFT ( $317.4 \pm 9.6$  mg/L). Further, because alum consumes alkalinity, the total alkalinity and bicarbonate concentrations are lower in PASS. Porewater aluminium concentrations in the FFT, PASS, and BCR water are not shown in Table 2 because they are below the detection limit of 0.001 mg/L. Given the pH of PASS, it is likely that the aluminium added during coagulation is precipitated as  $\text{Al}(\text{OH})_{3(s)}$ . All water chemistry parameters listed in Table 2 are lower in BCR water than in FFT and PASS, except for pH.

**Table 2 Characterisation of untreated FFT, PASS, and BCR water on Day 0. Results are presented as average  $\pm$  one standard deviation of triplicates. Modified from Cossey et al. (2021b)**

| Parameter  | FFT              | PASS             | BCR water        |
|--|------------------|------------------|------------------|
| Solids content (wt%)                                   | 33.5 $\pm$ 0.7   | 30.1 $\pm$ 0.0   | –                |
| Water content (wt%)                                    | 66.5 $\pm$ 0.6   | 69.9 $\pm$ 0.0   | –                |
| MBI (meq/100 g)  | 12.2 $\pm$ 0.6   | *                | –                |
| Clay content (dry wt% based on MBI)                    | 87.6 $\pm$ 4.1   | *                | –                |
| Sand to fines ratio (SFR) (wt/wt)                      | 0.07 $\pm$ 0.02  | *                | –                |
| D <sub>50</sub> (median particle diameter) ( $\mu$ m)  | 1.4 $\pm$ 0.1    | *                | –                |
| Bitumen content (wt%)                                  | 1.0 $\pm$ 0.0    | *                | –                |
| pH   | 7.3 $\pm$ 0.1    | 7.4 $\pm$ 0.2    | 8.4 $\pm$ 0.1    |
| EC ( $\mu$ S/cm)                                       | 761 $\pm$ 33     | 816 $\pm$ 8      | 357 $\pm$ 8      |
| Sodium, Na <sup>+</sup> (mg/L)                         | 230.0 $\pm$ 11.0 | 241.2 $\pm$ 2.4  | 43.0 $\pm$ 0.5   |
| Magnesium, Mg <sup>2+</sup> (mg/L)                     | 29.5 $\pm$ 1.9   | 39.7 $\pm$ 0.7   | 11.7 $\pm$ 0.5   |
| Calcium, Ca <sup>2+</sup> (mg/L)                       | 60.7 $\pm$ 0.5   | 85.2 $\pm$ 2.4   | 23.6 $\pm$ 0.4   |
| Chloride, Cl <sup>-</sup> (mg/L)                       | 14.7 $\pm$ 0.8   | 34.1 $\pm$ 1.1   | 7.5 $\pm$ 0.3    |
| Sulphate, SO <sub>4</sub> <sup>2-</sup> (mg/L)         | 317.4 $\pm$ 9.6  | 631.9 $\pm$ 21.4 | 21.7 $\pm$ 0.9   |
| Total sulphide species (as S <sup>2-</sup> in $\mu$ M) | 0.0 $\pm$ 0.0    | 0.0 $\pm$ 0.0    | 0.0 $\pm$ 0.0    |
| Total alkalinity (mg CaCO <sub>3</sub> /L)             | 415.8 $\pm$ 9.0  | 309.7 $\pm$ 4.2  | 148.8 $\pm$ 10.2 |
| Bicarbonate, HCO <sub>3</sub> <sup>-</sup> (mg/L)      | 510.6 $\pm$ 10.9 | 377.8 $\pm$ 5.2  | 181.6 $\pm$ 11.6 |
| DOC (mg/L)   | 54.8 $\pm$ 3.1   | 53.2 $\pm$ 0.2   | 19.2 $\pm$ 0.4   |
| NAFCs (mg/L)   | 62.3 $\pm$ 5.7   | 43.5 $\pm$ 10.6  | 2.4 $\pm$ 0.4    |

\*Values in PASS are assumed to be the same as the original FFT (although D<sub>50</sub> does not account for floc formation in PASS); however, these parameters were not measured independently in PASS.

Figure 2 shows the interface settlement at the tailings-water interface for each of the 40 columns (19 L columns in Figure 2a; 1 L columns in Figure 2b) over 240 d. Based on Figure 2, PASS appears to be settling and consolidating faster than comparable FFT columns, except for the FFT S10 and FFT S20 columns; by Day 240, FFT S10 and FFT S20 columns had higher interface settlement than PASS S10 and PASS S20 columns. Typically, chemically amending tailings with coagulants and flocculants leads to faster settlement and consolidation (dewatering); therefore, the behaviour seen in Figure 2 is not surprising (Li et al. 2021a; Wilson et al. 2018). However, during the PASS treatment process, both coagulant and polymer solutions are added to the FFT, increasing the initial water content of the tailings. As shown in Table 2, the initial water content for PASS was approximately 3.4 wt% higher than that of untreated FFT. Therefore, it is best to compare the settlement and consolidation behaviour of PASS and FFT in terms of net water release (NWR) (determined using Equation 1 (Amoako 2020)).

$$NWR = V_{wr} - V_p \quad (1)$$

where:

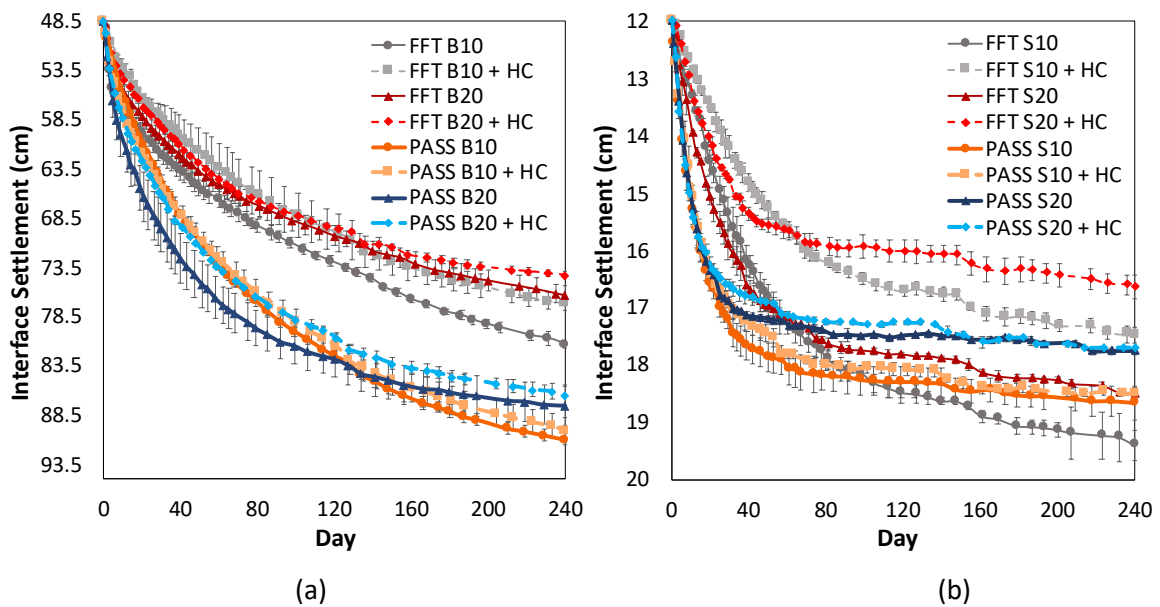
$NWR$  = net water release.

$V_{wr}$  = volume of water release.

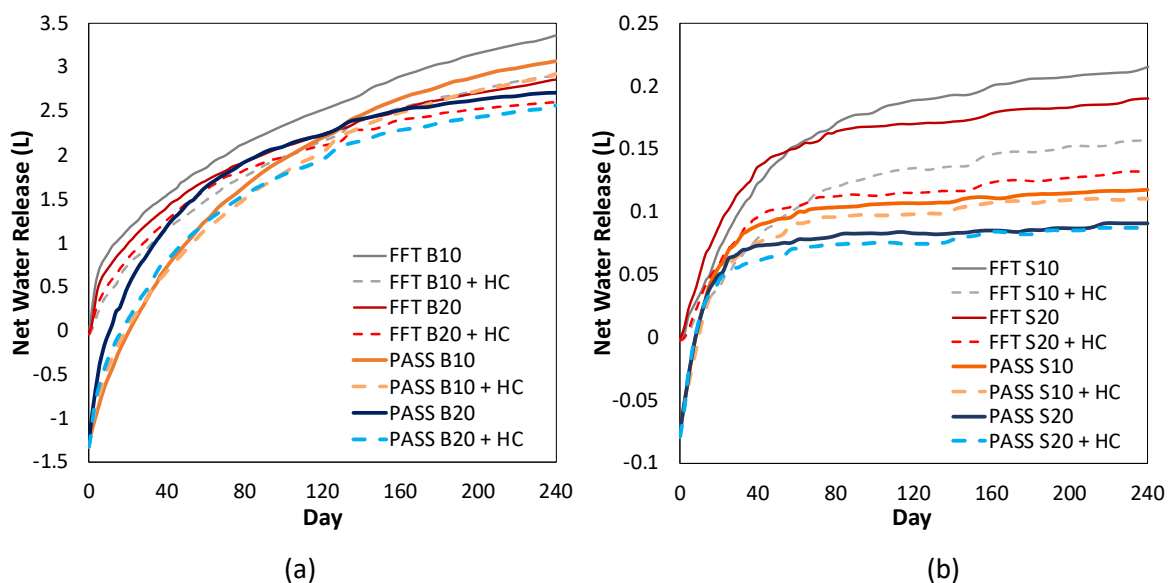
$V_p$  = volume of coagulant and polymer solutions added to FFT during treatment.

Figure 3 presents the NWR from PASS and FFT for all 40 columns (19 L columns shown in Figure 3a; 1 L columns in Figure 3b) over 240 d. Negative NWR values indicate the volume of coagulant and polymer

solutions remaining in the tailings. Positive NWR values indicate the volume of the original FFT water that has been released. While all PASS columns eventually had a positive NWR, the NWR of all PASS columns was less than that of comparable FFT columns on Day 240. This is surprising, as flocculating FFT with a neutral or anionic polymer (such as PAM) typically improves FFT dewatering, generating a higher NWR relative to that of untreated FFT during sedimentation and consolidation (Amoako 2020; Li et al. 2021a). The lower NWR in the PASS columns may be explained by below-optimal flocculation performance. Flocculation performance is dependent on numerous factors, including polymer dosage, mixing, and feed material properties (Li et al. 2021a). As shown in Table 2, the tailings used in this experiment have a high clay content of  $87.6 \pm 4.1$  dry wt% (based on MBI), which can negatively impact dewatering performance because of the water-holding capacity of clays (Li et al. 2021a). Further, the treatment used in this work was intentionally underdosed slightly as that has been found to reduce DOC in the release water. While typically this dosage would still be expected to deliver greater NWR than untreated FFT, it highlights challenges associated with achieving good flocculation conditions.



**Figure 2** Interface settlement in (a) 16 19 L columns and (b) 24 1 L columns. Results are averages of (a) duplicate or (b) triplicate columns, and error bars represent one standard deviation of replicates



**Figure 3** Net water release in (a) 16 19 L columns and (b) 24 1 L columns. Results are averages of (a) duplicate or (b) triplicate columns



The effects of column shape and size on interface settlement can be seen in Table 3, which presents the percent interface settlement in the 40 columns on Day 240. FFT and PASS in the 1 L columns are settling and consolidating at faster rates than FFT and PASS in the 19 L columns, with average interface settlements of  $39.9 \pm 5.6\%$  and  $28.3 \pm 5.4\%$  for 1 L and 19 L columns, respectively, by Day 240. The 1 L columns have a cross-sectional area 0.3 times that of the 19 L columns, which might suggest that the 1 L columns should have lower interface settlement rates due to wall effects (friction), although this is not the case (Baotian et al. 2013; Gao et al. 2016). Instead, the most likely explanation for the faster settling and consolidation behaviour in the smaller columns is that the smooth column walls are acting as a less tortuous, preferential flow path or short circuit for porewater moving from the tailings into the water cap (Comiti & Renaud 1989; Sentenac et al. 2001). The larger column surface area per volume of tailings in the 1 L columns ( $639 \text{ cm}^2/\text{L}$  of tailings) than the 19 L columns ( $350 \text{ cm}^2/\text{L}$  of tailings) and the higher interface settlement rates in the 1 L columns are consistent with the preferential flow path explanation.

**Table 3** Percent interface settlement for 40 columns on Day 240. Results are presented as averaged  $\pm$  one standard deviation of replicates. 19 L column results are averages of duplicates; 1 L column results are averages of triplicates

| Column       | Size           |                |
|--------------|----------------|----------------|
|              | Big (19 L)     | Small (1 L)    |
| FFT 10       | $26.9 \pm 0.3$ | $48.5 \pm 1.7$ |
| FFT 10 + HC  | $23.5 \pm 0.6$ | $35.9 \pm 0.8$ |
| FFT 20       | $22.8 \pm 0.8$ | $42.8 \pm 0.7$ |
| FFT 20 + HC  | $21.1 \pm 0.3$ | $30.4 \pm 1.3$ |
| PASS 10      | $34.8 \pm 0.5$ | $43.7 \pm 2.0$ |
| PASS 10 + HC | $34.0 \pm 1.0$ | $42.6 \pm 0.7$ |
| PASS 20      | $32.0 \pm 1.6$ | $37.8 \pm 0.4$ |
| PASS 20 + HC | $31.1 \pm 0.9$ | $37.4 \pm 0.0$ |

The effects of temperature and hydrocarbon amendments on tailings settlement and consolidation are not as apparent, though, in general, higher temperature and hydrocarbon amendments appear to result in slower settlement and consolidation. This is an interesting observation because higher temperature should increase hydraulic conductivity and thereby self-weight consolidation. Further, microbial activity is enhanced by higher temperature and hydrocarbon amendments, which have previously been found to result in bioconsolidation of FFT through the release and dissolution of biogenic gases (Siddique et al. 2014b). While biogenic gases are visibly trapped in the FFT and PASS amended with hydrocarbons and/or stored at  $20^\circ\text{C}$ , as of Day 240 the hydrocarbon amendments and higher temperature have not led to the bioconsolidation phenomenon noted by Siddique et al. (2014b). The discrepancy between the findings of this study and those of Siddique et al. (2014b) may be because of (i) different tailings sources and thereby microbial communities; (ii) different carbon amendments, as the hydrocarbons used in this work are not as labile as the canola meal hydrolysate used by Siddique et al. (2014b); (iii) the higher clay content of the FFT used in this work, which may hinder gas ebullition; and (iv) the FFT used by Siddique et al. (2014b) was diluted to achieve a solids content of 23.4 wt%, making the FFT weaker and therefore making it easier for gas bubbles to escape.

Figure 4 presents sodium ( $\text{Na}^+$ ) concentrations in the water cap of all 40 columns from Day 0 to 240 (19 L columns shown in Figure 4a; 1 L columns in Figure 4b). Sodium is the cation with the highest concentration in the FFT and PASS porewater and is also the cation with the highest concentration in the column water caps. The trends seen in Figure 4 are generally consistent with the consolidation trends seen in Figures 2 and 3 and thus can be attributed to advective fluxes of FFT and PASS porewater into the water caps. Sodium fluxes into the water caps were highest initially but appear to be slowing over time in the

1 L columns. This is consistent with the plateaus in interface settlement (Figure 2b) and NWR (Figure 3b) occurring in the 1 L columns and is to be expected as consolidation rates decrease over time (COSIA 2021). Water cap concentrations of other cations, anions, and alkalinity (data not shown) are also increasing over time in all columns, consistent with the consolidation trends seen in Figures 2 and 3. This work suggests that salt fluxes from PASS and FFT are similar. While the PASS technology is expected to improve the quality of expressed porewater (COSIA 2021), it is likely through the reduction of suspended solids and residual organic matter (bitumen) in the water cap rather than reduced dissolved salts. However, preliminary results up to Day 240 indicate that DOC concentrations in the water caps are similar in columns containing FFT or PASS and depend not only on consolidation trends but also on microbial activity.

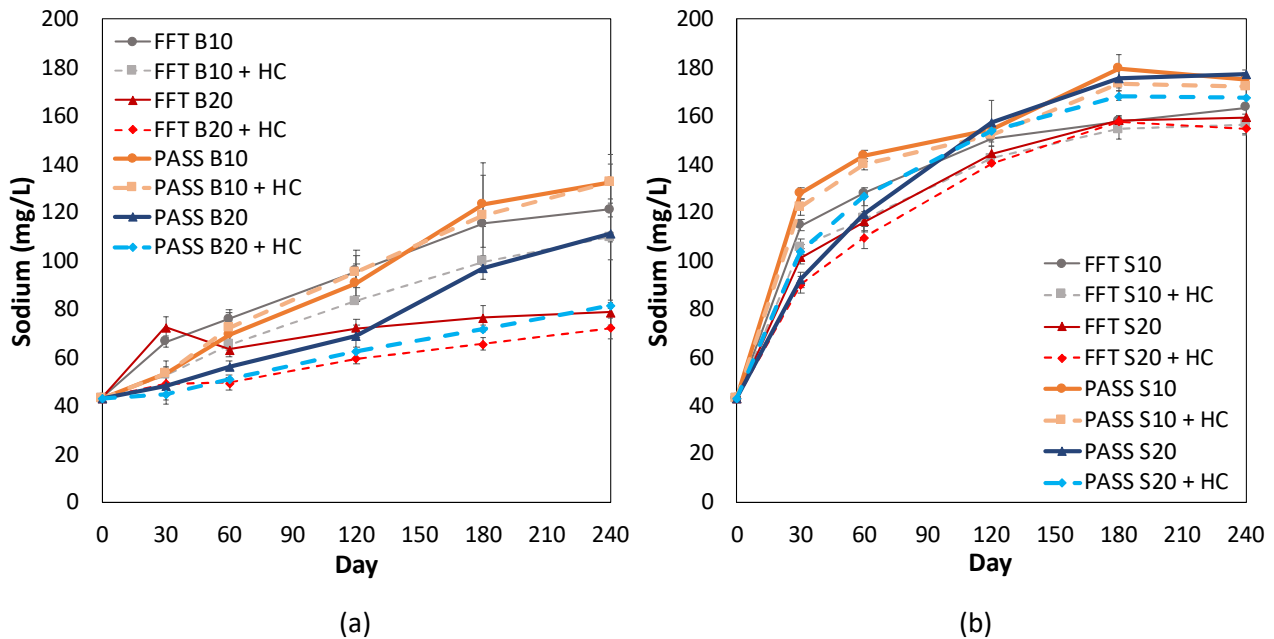


**Figure 4** Water cap sodium concentrations in (a) 16 19 L columns and (b) 24 1 L columns. Results are averaged from (a) duplicate or (b) triplicate columns and error bars represent one standard deviation of replicates

To date, water cap samples from all 40 columns have had aluminium concentrations either below detection or below the applicable Alberta Surface Water Quality Guidelines for the protection of aquatic life (Government of Alberta 2018). Further, PAM concentrations in the Day 180 water cap samples from the 19 L columns were below detection (<10 mg/L). The FFT and PASS porewater samples measured on Day 0 also did not have detectable concentrations of PAM; therefore, PAM is likely residing in the solid phase and sorbing to the mineral surfaces.

Figure 5 displays the porewater sulfate ( $\text{SO}_4^{2-}$ ) concentrations in the 16 19 L columns from Day 0 to 240. Most of the sulfate reduction occurred within the first 120 days of the experiment, where sulfate concentrations were reduced on average by 96% (304 mg/L) for FFT amended with hydrocarbons and 93% (589 mg/L) for PASS amended with hydrocarbons. For FFT and PASS without hydrocarbon amendments, sulfate concentrations were reduced on average by 3% (9 mg/L) and 27% (175 mg/L), respectively, by Day 120. Hydrocarbon amendments have had the largest impact on sulfate reduction rates, though columns stored at 20°C also have higher sulfate reduction rates than columns stored at 10°C. Further, columns containing PASS have undergone more extensive sulfate reduction than columns containing FFT.

To determine the fate of reduced sulfur species generated during sulfate reduction (Figure 5), headspace and porewater samples collected from the 16 19 L columns were analysed for gaseous  $\text{H}_2\text{S}$  and aqueous total sulfide species ( $\text{H}_2\text{S}$ ,  $\text{HS}^-$ ,  $\text{S}^{2-}$ ), respectively.  $\text{H}_2\text{S}$  was below detection (<0.1 ppmv) in all headspace samples collected on Day 180, except in one of the PASS B10 + HC columns, which had an  $\text{H}_2\text{S}$  concentration of

2.5 ppmv. As previously mentioned, it is possible that H<sub>2</sub>S gas bubbles are trapped in the tailings rather than escaping to the headspace.

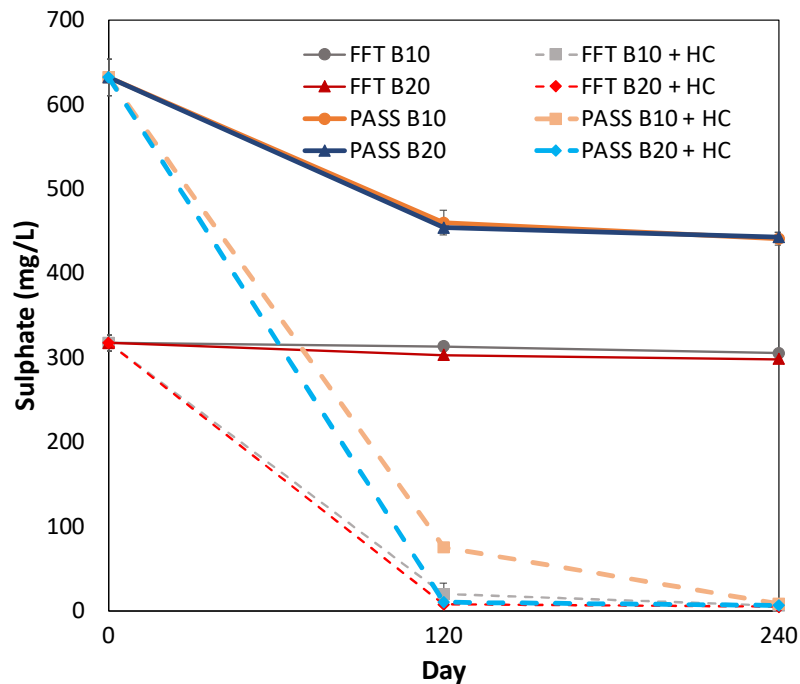


**Figure 5 Porewater sulfate concentrations in 19 L columns. Results are averaged from duplicate columns and error bars represent one standard deviation of duplicates**

Porewater total sulfide species (as S<sup>2-</sup>) concentrations in the 19 L columns on Days 120 and 240 are presented in Figure 6. Note that Day 0 porewater samples of FFT and PASS did not have sulfide species present. Further, given the circumneutral pH of the FFT and PASS, the aqueous sulfide species present will primarily be HS<sup>-</sup> and H<sub>2</sub>S. Aqueous total sulfide species are highest in PASS B10 + HC and PASS B20 + HC, and these are also the columns that have undergone the most extensive sulfate reduction. These findings suggest that sulfate reduction should be carefully considered when applying PASS treatment to froth treatment tailings, as the additional carbon sources in froth treatment tailings may substantially increase sulfate reduction and the generation of sulfide species. However, total sulfide species concentrations in the porewater are highly variable, as indicated by the large error bars in Figure 6. Measuring aqueous total sulfide species is time sensitive; however, tailings samples must be centrifuged prior to extracting porewater and measuring sulfide species concentrations. As a result, the concentrations presented in Figure 6 are highly variable and likely underestimated. Aqueous sulfide species are also present in the water caps of the 19 L columns, although in all almost columns, the water cap concentrations of total sulfide species are lower than the concentrations presented in Figure 6. The gaseous and aqueous sulfur species measured in the headspace and water samples account for only a fraction of the reduced sulfur that would be generated by the sulfate reduction seen in Figure 5. As such, some reduced sulfur species are likely precipitating as metal sulfides, such as FeS<sub>(s)</sub>, given the anaerobic conditions in the columns. The photos of FFT and PASS columns in Figure 1 were taken on Day 120, and the black colour observed in the FFT B10 + HC tailings and the PASS S10 tailings is indicative of FeS<sub>(s)</sub> formation.

As of Day 240, low levels of CO<sub>2</sub> are present in the headspaces of all 40 columns, which is consistent with sulfate reduction and microbial activity in general; however, CH<sub>4</sub> is below detection (0.16%) in all columns. This indicates that methanogenesis has not yet started in the FFT and PASS, although it can take years for these microbial communities to develop in fresh oil sands tailings and produce CH<sub>4</sub> (Foght et al. 2017).

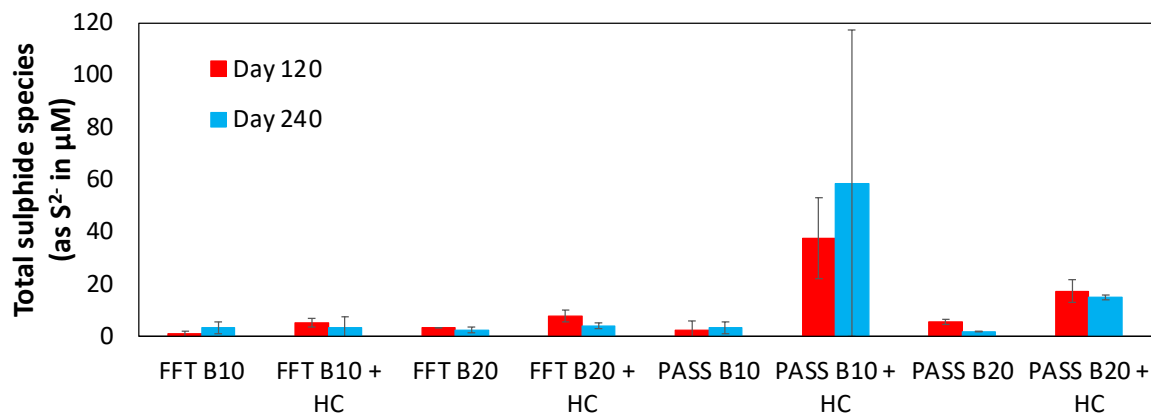


**Figure 6** Porewater total sulfide species concentrations in 19 L columns. Results are averaged from duplicate columns and error bars represent one standard deviation of duplicates

## 4 Conclusion

Results to date highlight important differences in the biogeochemical and geotechnical behaviour of FFT and PASS in EPLs. In almost all cases, interface settlement is highest in columns containing PASS. However, because PASS results in a lower NWR than FFT, the PASS treatment is not improving the dewatering performance of the tailings in this case. As such, field data should be carefully reviewed to ensure that dewatering performance is improving with time after PASS treatment. As expected, fluxes of salts into the column water caps are generally consistent with consolidation trends and are similar for columns containing either FFT or PASS. Most of the sulfate reduction observed in the columns occurred within the first 120 d, and columns containing PASS and/or hydrocarbon amendments have undergone the most extensive sulfate reduction. As a result, sulfide species are present throughout the tailings and water caps in all columns, with concentrations ranging from 0.8 to 7.8 µM and 1.7 to 58.6 µM in FFT and PASS, respectively.

## Acknowledgement

The authors are grateful for research support from the NSERC/COSIA Industrial Research Chair in Oil Sands Tailings Geotechnique (IRCPJ 460863 – 18). As well, the authors are grateful for support from the NSERC/COSIA Industrial Research Chair for Colleges in Oil Sands Tailings Management (CIRC 534019-18), which supported the team at NAIT in conducting the characterisation and flocculation work. H Cossey is also grateful for financial support from the Vanier-Banting Secretariat in completing this project. Finally, the authors would like to thank Dr P Kuznetsov, Dr MN Anwar, and Amy-lyne Balaberda at the University of Alberta and Dr Yunhui Li and Mohammed Ghuzi at NAIT for their guidance and assistance in conducting this research.

## References

- Alberta Energy Regulator 2021, *State of Fluid Tailings Management for Mineable Oil Sands, 2020*, Alberta Energy Regulator, Calgary.
- ASTM 2017, *Standard Test Method for Particle-Size Distribution (Gradation) of Fine-grained Soils Using the Sedimentation (Hydrometer) D7928-17*, ASTM International, West Conshohocken.
- Amoako, KA 2020, *Geotechnical Behaviour of Two Novel Polymer Treatments of Oil Sands Fine Tailings*, MSc Thesis, University of Alberta, Edmonton.
- Baotian, W, Shuaijie, G & Funhai, Z 2013, 'Research on deposition and consolidation behavior of cohesive sediment with settlement column experiment', *European Journal of Environmental and Civil Engineering*, vol. 17, pp. s144–s157.
- Brown, LD & Ulrich, AC 2015, 'Oil sands naphthenic acids: a review of properties, measurement, and treatment', *Chemosphere*, vol. 127, pp. 276–290.
- Burkus, Z, Wheler, J & Pletcher, S 2014, *GHG Emissions from Oil Sands Tailings Ponds: Overview and Modelling Based on Fermentable Substrates. In Part I: Review of Tailings Pond Facts and Practices*, Alberta Environment and Sustainable Resource Development, Edmonton.
- Canada's Oil Sands Innovation Alliance 2021, *Pit Lakes: A Surface Mining Perspective*, Canada's Oil Sands Innovation Alliance, Calgary.

- Clark, MG, Drewitt, GB & Carey, SK 2021, 'Energy and carbon fluxes from an oil sands pit lake', *Science of the Total Environment*, vol. 752, article no. 141966.
- Chalaturnyk, RJ, Scott, JD & Özüm, B 2002, 'Management of oil sands tailings', *Petroleum Science and Technology*, vol. 20, pp. 1025–1046.
- Comiti, J & Renaud, M 1989, 'A new model for determining mean structure parameters of fixed beds from pressure drop measurements, with application to beds packed with parallelepipedal particles', *Chemical Engineering Science*, vol. 44, pp. 1539–1545.
- Cossey, HL, Batycky, AE, Kaminsky, H & Ulrich, AC 2021a, 'Geochemical stability of oil sands tailings in mine closure landforms', *Minerals*, vol. 11, article no. 830.
- Cossey, HL, Kuznetsov, PV & Ulrich, AC 2021b, 'Evaluating the biogeochemical and consolidation behavior of oil sands end pit lakes with accelerated aging', in NA Beier, GW Wilson & DC Segó (eds), *Proceedings of 25th International Conference on Tailings and Mine Waste*, University of Alberta Geotechnical Center & Oil Sands Tailings Research Facility, Edmonton, pp. 793–802.
- Dompierre, KA, Lindsay, MJB, Cruz-Hernández, P & Halferdahl, GM 2016, 'Initial geochemical characteristics of fluid fine tailings in an oil sands end pit lake', *Science of the Total Environment*, vol. 556, pp. 196–206.
- Foght, JM, Gieg, LM & Siddique, T 2017, 'The microbiology of oil sands tailings: past, present, future', *FEMs Microbiology Ecology*, vol. 93, article no. fix034.
- Gao, YF, Zhang, Y, Zhou, Y & Li, D 2016, 'Effects of column diameter on settling behavior of dredged slurry in sedimentation experiments', *Marine Georesources & Geotechnology*, vol. 34, pp. 431–439.
- Gee, K, Poon, HY, Hashisho, Z & Ulrich, AC 2017, 'Effect of naphtha diluent on greenhouse gases and reduced sulfur compounds emissions from oil sands tailings', *Science of the Total Environment*, vol. 598, pp. 916–924.
- Government of Alberta 2018, *Environmental Quality Guidelines for Alberta Surface Water*, Alberta Environment and Parks, Water Branch, Edmonton.
- Government of Alberta, 2022, Government of Alberta, Edmonton, viewed 18 March 2022, <http://environment.alberta.ca/apps/EdwReportViewer/LongTermRiverStation.aspx>
- Jessen, GL, Chen, LX, Mori, JF, Colenbrander Nelson, TE, Slater, GF, Lindsay, MJB, ... Warren, LA 2022, 'Alum addition triggers hypoxia in engineered pit lake', *Microorganisms*, vol. 10, article no. 510.
- Kaminsky, H 2014, 'Demystifying the methylene blue index', *Proceedings of the 4th International Oil Sands Tailings Conference*, University of Alberta Geotechnical Center & Oil Sands Tailings Research Facility, Banff.
- Li, Y, Kaminsky, H, Gong, XY, Sun, YS., Ghuzi, M & Sadighian, A 2021a, 'What affects dewatering performance of high density slurry?', *Minerals*, vol. 11, article no. 761.
- Li, Y, Kaminsky, H, Romero, C, Gong, XY, Ghuzi, M & Tacas, J 2021b, 'Assessing dewatering performance of treated fluid fine tailings with a bench-scale filter press', in NA Beier, GW Wilson & DC Segó (eds), *Proceedings of 25th International Conference on Tailings and Mine Waste*, University of Alberta Geotechnical Center & Oil Sands Tailings Research Facility, Edmonton, pp. 862–872.
- Li, Y, Kaminsky, H, Sadighian, A, Sun, YS, Murphy, F, Gong, XY, Ghuzi, M & Rima, U 2022, 'Impact of chemical and physical treatments on freeze-thaw dewatering of fluid fine tailings', *Cold Regions Science and Technology*, vol. 193, article no. 103385.
- Monaghan, J, Richards, LC, Vandergrift, GW, Hounjet, LJ, Stoyanov, SR, Gill, CG & Krogh, ET 2021, 'Direct mass spectrometric analysis of naphthenic acids and polycyclic aromatic hydrocarbons in waters impacted by diluted bitumen and conventional crude oil', *Science of the Total Environment*, vol. 765, article no. 144206.
- Pavlostathis, SG & Zhuang, P 1991, 'Effect of temperature on the development of anaerobic cultures from a contaminated subsurface soil', *Environmental Technology*, vol. 12, pp. 679–687.
- Ramos-Padrón, E, Bordenave, S, Lin, S, Bhaskar, IM, Dong, X, Sensen, CW, Fournier, J, Vourdouw, G & Gieg, LM 2011, 'Carbon and sulfur cycling by microbial communities in a gypsum-treated oil sands tailings pond', *Environmental Science & Technology*, vol. 45, pp. 439–446.
- Reid, ML & Warren, LA 2016, 'S reactivity of an oil sands composite tailings deposit undergoing reclamation wetland construction', *Journal of Environmental Management*, vol. 166, pp. 321–329.
- Ripmeester, MJ & Duford, DA 2019, 'Method for routine "naphthenic acids fraction compounds" determination in oil sands process affected water by liquid-liquid extraction in dichloromethane and Fourier-Transform Infrared Spectroscopy', *Chemosphere*, vol. 233, pp. 687–696.
- Rundle, KI, Sharaf, MS, Stevens, D, Kamunde, C & van der Heuvel, MR 2018, 'Oil sands derived naphthenic acids are oxidative uncouplers and impair electron transport in isolated mitochondria', *Environmental Science & Technology*, vol. 765, pp. 10810–10811.
- Sentenac, P, Lynch, RJ & Bolton, MD 2001, 'Measurement of a side-wall boundary effect in soil columns using fibre-optics sensing', *International Journal of Physical Modelling in Geotechnics*, vol. 4, pp. 35–41.
- Siddique, T, Fedorak, PM & Foght, JM 2006, 'Biodegradation of short-chain n-alkanes in oil sands tailings under methanogenic conditions', *Environmental Science & Technology*, vol. 40, pp. 5459–5464.
- Siddique, T, Fedorak, PM, Mackinnon, MD & Foght, JM 2007, 'Metabolism of BTEX and naphtha compounds to methane in oil sands tailings', *Environmental Science & Technology*, vol. 41, pp. 2350–2356.
- Siddique, T, Kuznetsov, P, Kuznetsova, A, Li, C, Young, R, Arocena, JM & Foght, JM 2014a, 'Microbially-accelerated consolidation of oil sands tailings. Pathway II: solid phase biogeochemistry', *Frontiers in Microbiology*, vol. 5, article no. 107.
- Siddique, T, Kuznetsov, P, Kuznetsova, A, Arkell, N, Young, R, Li, C, Guigard, S, Underwood, E & Foght, JM 2014b, 'Microbially-accelerated consolidation of oil sands tailings. Pathway I: changes in porewater chemistry', *Frontiers in Microbiology*, vol. 5, article no. 106.

- Siddique, T, Mohamad Shahimin, MF, Zamir, S, Semple, K, Li, C & Foght, JM 2015, 'Long-term incubation reveals methanogenic biodegradation of C5 and C6 iso-alkanes in oil sands tailings', *Environmental Science & Technology*, vol. 49, pp. 14732–14739.
- Siddique, T, Penner, T, Semple, K & Foght, JM 2011, 'Anaerobic biodegradation of longer-chain n-alkanes coupled to methane production in oil sands tailings', *Environmental Science & Technology*, vol. 45, pp. 5892–5899.
- Siddique, T, Semple, K, Li, C & Foght, JM 2020, 'Methanogenic biodegradation of iso-alkanes and cycloalkanes during long-term incubation with oil sands tailings', *Environmental Pollution*, vol. 258, article no. 113768.
- Small, CC, Cho, S, Hashisho, Z & Ulrich, AC 2015, 'Emissions from oil sands tailings ponds: Review of tailings pond parameters and emission estimates', *Journal of Petroleum Science and Engineering*, vol. 127, pp. 490–501.
- Stasik, S, Loick, N, Knöller, K, Weisener, C & Wendt-Potthoff, K 2014, 'Understanding biogeochemical gradients of sulfur, iron and carbon in an oil sands tailings pond', *Chemical Geology*, vol. 382, pp. 44–53.
- Stasik, S & Wendt-Potthoff, K 2014, 'Interaction of microbial sulphate reduction and methanogenesis in oil sands tailings ponds', *Chemosphere*, vol. 103, pp. 59–66.
- Syncrude Canada Ltd 2020, *2019 Mildred Lake Tailings Management Report*, Syncrude Canada Ltd, Fort McMurray.
- Syncrude Canada Ltd 2021, *2021 Pit Lake Monitoring and Research Report (Base Mine Lake Demonstration Summary: 2021-2020)*, Syncrude Canada Ltd, Fort McMurray.
- Tedford, E, Halferdahl, G, Pieters, R & Lawrence, GA 2019, 'Temporal variations in turbidity in an oil sands pit lake', *Environmental Fluid Mechanics*, vol. 19, pp. 457–473.
- Warren, LA, Kendra, KE, Brady, AL & Slater, GF 2016, 'Sulfur biogeochemistry of an oil sands composite tailings deposit', *Frontiers in Microbiology*, vol. 6, pp. 1–14.
- White, KB & Liber, K 2018, 'Early chemical and toxicological risk characterization of inorganic constituents in surface water from the Canadian oil sands first large-scale end pit lake', *Chemosphere*, vol. 211, pp. 745–757.
- White, KB & Liber, K 2020, 'Chronic toxicity of surface water from a Canadian oil sands end pit lake to the freshwater invertebrates *Chironomus dilutus* and *Ceriodaphnia dubia*', *Archives of Environmental Contamination and Toxicology*, vol. 78, pp. 439–450.
- Wilson, GW, Kabwe, LK, Beier, NA & Scott, JD 2018, 'Effect of various treatments on consolidation of oil sands fluid fine tailing', *Canadian Geotechnical Journal*, vol. 55, pp. 1059–1066.
- Wong, M, An, D, Caffrey, SM, Soh, J, Dong, X, Sensen, CW, Oldenburg, TBP, Larter, SR & Voordouw, G 2015, 'Roles of thermophiles and fungi in bitumen degradation in mostly cold oil sands outcrops', *Applied and Environmental Microbiology*, vol. 81, pp. 6825–6838.